2020 American Control Conference
Denver, CO, USA, July 1-3, 2020

Analysis of Online Parameter Estimation for Electrochemical Li-ion Battery Models via Reduced Sensitivity Equations

Zachary T. Gima[1], Dylan Kato[1], Reinhardt Klein[2], Scott J. Moura[1]

Abstract— **This paper focuses on the problem of online parameter estimation in an electrochemical Li-ion battery model. Online parameter estimation is necessary to account for model mismatch, environmental disturbances, and cycle-induced aging in Li-ion battery models. Sensitivity analysis can improve parameter estimation by identifying which data the parameters are most sensitive to. However, computing parameter sensitivity in full-order electrochemical models is typically intractable for online applications. Using a reduced-order model can lower the computational burden and, as we demonstrate, approximates well the sensitivity of the higher-order model. To provide further insight into the parameter estimation challenge, we analyze the effect that identifying parameters according to voltage RMSE data has on internal state errors. We perform a simulation study which demonstrates that parameter estimation approaches based on this paradigm are not sufficient for safe battery operation or other control objectives that require accurate estimates of these states.**

I. INTRODUCTION

Batteries are an essential technology for applications ranging from mobile electronics to electrified transportation. Battery management systems (BMS) enable these applications by monitoring the battery's condition and facilitating charging and discharging according to the system demands. Throughout operation, a critical role of the BMS is to accurately estimate and update the model states and parameters. Lack of identifiability in electrochemical models makes parameter estimation a fundamentally challenging problem [1], [2]. Further complicating the problem, battery cycling naturally causes performance degradation which manifests as changing model parameter values. Typically, existing research address these issues by exploring novel modeling and/or parameter estimation schemes [3], [4], [5].

In other applications [6], [7] and more recently the battery modeling and controls community [8], [9], [2] researchers have explicitly considered the information content, i.e. the parameter sensitivity, for parameter estimation. While several works have explored sensitivity analysis for optimal experiment design (OED) and offline model parameterization [10], [11], [12], here we focus on the less-explored online parameter estimation problem. As [8] first illustrated, sensitivity analysis can enhance online parameter estimation by screening incoming data and only using data subsets that maximize parameter sensitivity.

[1]Zachary T. Gima, Dylan Kato, and Prof. Scott J. Moura are with the Energy, Controls and Applications Lab (eCAL), University of California, Berkeley, CA 94720, USA {ztakeo, dkkato, smoura}@berkeley.edu)

[2]Reinhardt Klein is with Robert Bosch LLC, Research and Technology Center, Sunnyvale, CA 94085 USA reinhardt.klein@us.bosch.com)

One practical challenge of evaluating the sensitivity in electrochemical battery models is computational complexity. The complexity grows intractable for full-order electrochemical battery models, which have hundreds or thousands of states and are highly nonlinear in the parameters. Furthermore, many applications such as electric vehicle operation generate too much data to compute all of the sensitivity content. Limited work has attempted to address this fundamental limitation. Reference [9] addresses this problem and lowers computational burden by deriving analytic sensitivity expressions for a given set of parameters in a single particle model (SPM). The work showed good agreement between analytic and numerical sensitivity results. However, the approach requires deriving sensitivity expressions by-hand for each parameter. Additionally, approximating and discretizing these expressions for implementation may limit their accuracy.

Using a reduced-order electrochemical model to compute sensitivity information and then estimate parameters in the full-order model is an attractive alternative because several well-studied options exist, such as the SPM, SPM with electrolyte dynamics (SPMe), and other variants. Furthermore, sensitivity calculations via automatic differentiation for reduced-order models can be sufficiently fast for some online applications. As we will show, using a reduced-order electrochemical model can approximate the sensitivity of the higher-order model across a wide range of inputs.

Sensitivity-based approaches have been shown to improve parameter estimation in terms of reduced voltage RMSE and improved identification speed. However, minimal work has explored the effect of parameter estimation using voltage RMSE on internal state estimation. Accurate internal state estimates are critical in applications such as fast charging. To study this problem, we perform an analysis on a parameter estimation approach that (1) leverages the reduced-order electrochemical models to perform efficient sensitivity computations for selecting the optimal data for parameter estimation; and (2) uses the subset of optimal data to estimate parameters in the full-order model. We demonstrate that fitting solely to voltage sacrifices safety. We summarize our key contributions next.

Key contributions of the work presented here include: (1) Analysis of using reduced-sensitivity equations to fit parameters of the full-order model and (2) increased understanding of parameter estimation and safety trade-offs in electrochemical models by highlighting that minimizing measured voltage error does not minimize internal state error.

The rest of the paper is organized as follows. Section

978-1-5386-8266-1/$31.00 ©2020 AACC

II describes the electrochemical battery model equations. Section III explains sensitivity analysis and the connection with the parameter estimation framework we define. Section IV details the model-to-model comparison setup used to evaluate the validity of our approach. In Section V we present our simulation results and interpret our findings. Finally, in Section VI we summarize and detail possible future research directions.

II. ELECTROCHEMICAL BATTERY MODEL

In this section, we describe the electrochemical battery models of relevance to this work. To balance accuracy and computational tractability, our framework uses the Single Particle Model with Electrolyte & Thermal (SPMeT) dynamics as developed in [13], [14] to compute sensitivity trajectories; for greater modeling fidelity, we simulate and continually update the parameters in the "full-order" Doyle-Fuller-Newman (DFN) model. The derivation and theoretical underpinning of these models are well studied and commonly used. For the sake of brevity, we provide a brief summary of the SPMeT equations here. We refer the reader to [15] for the DFN model equations and derivation.

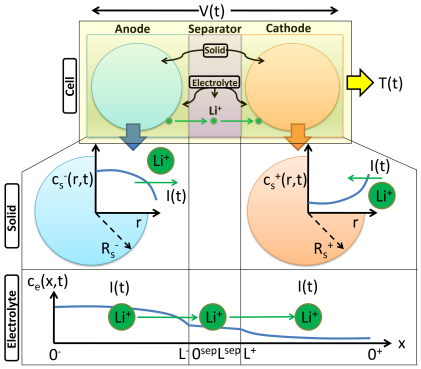

Fig. 1: SPMe visual representation [14]. This view details a cross section of a typical Li-ion cell, consisting of three sections from left to right: anode, separator, cathode. The model considers dynamics for two phases of material: solid and electrolyte. Collapsing the spatial dimension x used in the DFN, the solid phase evolves only in the r dimension. The electrolyte states evolve in the x dimension.

The SPMeT consists of four sets of equations:

1) Two linear spherical diffusion PDEs (positive & negative electrode) modeling each electrode's solid concentration dynamics:

$$\frac{\partial \bar{c}_s^{\pm}}{\partial t}(r,t) = \frac{1}{r^2}\frac{\partial}{\partial r}\left[D_s^{\pm} r^2 \frac{\partial \bar{c}_s^{\pm}}{\partial r}(r,t)\right] \tag{1}$$

2) A quasilinear diffusion equation (across three domains: cathode, separator, anode) modeling the electrolyte concentration dynamics:

$$\frac{\partial c_e^{\pm}}{\partial t}(x,t) = \frac{\partial}{\partial x}\left[D_e(c_e^{\pm})\frac{\partial c_e^{\pm}}{\partial x}(x,t)\right] \mp \frac{(1-t_c^0)}{\varepsilon_e^{\pm} F L^{-}} I(t) \tag{2}$$

$$\frac{\partial c_e^{sep}}{\partial t}(x,t) = \frac{\partial}{\partial x}\left[D_e(c_e^{sep})\frac{\partial c_e^{sep}}{\partial x}(x,t)\right] \tag{3}$$

3) A nonlinear output function mapping boundary values of solid concentration, electrolyte concentration, and current to terminal voltage:

$$\begin{aligned} V(t) = {} & \frac{RT(t)}{\alpha F}\sinh^{-1}\left(\frac{I(t)}{2a^{+}L^{+}+\bar{i}_0^{+}(t)}\right) \\ & - \frac{RT(t)}{\alpha F}\sinh^{-1}\left(\frac{-I(t)}{2a^{-}L^{-}+\bar{i}_0^{-}(t)}\right) \\ & + U^{+}(c_{ss}^{+}(t)) - U^{-}(c_{ss}^{-}(t)) \\ & + \left(\frac{R_f^{+}}{a^{+}L^{+}} + \frac{R_f^{-}}{a^{-}L^{-}}\right) I(t) \\ & - \frac{L^{+}+2L^{sep}+L^{-}}{2\bar{\kappa}} I(t) \\ & + k_{conc}(t)[\ln c_e(0^{+},t) - \ln c_e(0^{-},t)] \end{aligned} \tag{4}$$

4) Core & surface temperature ODEs:

$$\frac{\partial T_c(t)}{\partial t} = \frac{T_s(t)-T_c(t)}{R_c C_c} + \frac{\dot{Q}(t)}{C_c} \tag{5}$$

$$\frac{\partial T_s(t)}{\partial t} = \frac{T_f(t)-T_s(t)}{R_u C_s} - \frac{T_s(t)-T_c(t)}{R_c C_s} \tag{6}$$

The seven state variables x are lithium concentration in the solid $c_s^{\pm}(r,t)$ (two), lithium concentration in the electrolyte $c_e^{\{\pm,sep\}}(x,t)$ (three), and the core and surface temperatures $T_c(t), T_s(t)$ (two). Voltage $V(t)$ represents the lone measured output y.

III. SENSITIVITY-BASED DATA SELECTION AND PARAMETER ESTIMATION FRAMEWORK

This section lays out the general theory for the sensitivity analysis that underpins much of this work and explains the framework used for parameter estimation. The methodology is described visually in Figure 2.

A. Sensitivity Analysis & Data Selection

Sensitivity represents a fundamental property related to the information quality of signals. For signals that generate high parameter sensitivity, it can be shown that parameter estimates converge exponentially fast [16]. The method we present here directly evaluates the local sensitivity of the model input-output data to improve parameter estimation. As demonstrated in previous work [11] and by reference [8], data selection based on sensitivity content can improve parameter estimation accuracy and speed. Selecting data with higher sensitivity content enhances parameter estimation by better conditioning the Hessian of the objective function. We leverage that insight here to reduce the number of data sets used in estimating the parameters, selecting only the most informative input-output profiles and disregarding the rest. We describe the basic formulation of our framework below.

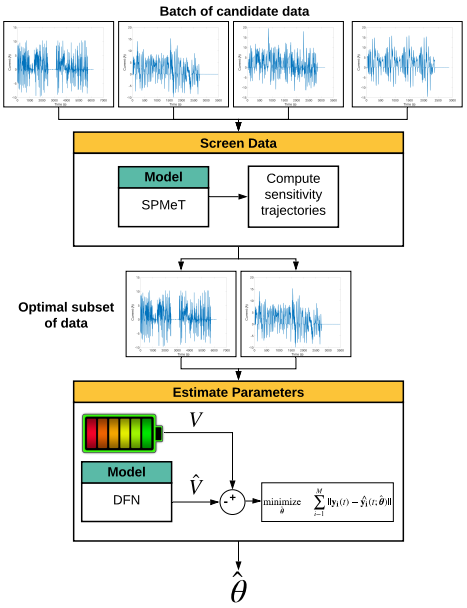

Fig. 2: Sensitivity-based data selection for parameter estimation methodology.

From the SPMeT equations presented in Section II, we can formulate an ordinary differential system of equation (ODEs) with the following form:

$$\dot{\mathbf{x}} = \boldsymbol{f}(\mathbf{x}, u, \boldsymbol{\theta}), \quad \mathbf{x}(t_0) = \mathbf{x_0}, \tag{7}$$

$$\mathbf{y} = \boldsymbol{h}(\mathbf{x}, \mathbf{u}, \boldsymbol{\theta}), \tag{8}$$

where $\mathbf{x} = [c_s^{\pm}, c_e^{\pm,sep}, T_c, T_s]^T$, $\mathbf{y} = V(t)$, and $\boldsymbol{\theta} = [R_s^+, \kappa, \varepsilon_e^-, t_+, R_f^+, R_f^-]$. Now, taking partial derivatives, define the following sensitivity variables:

$$S_{\mathbf{x}} = \frac{\partial \mathbf{x}}{\partial \boldsymbol{\theta}}, \quad S_{\mathbf{y}} = \frac{\partial \mathbf{y}}{\partial \boldsymbol{\theta}}, \tag{9}$$

where $S_{\mathbf{x}}$, $S_{\mathbf{y}}$ correspond to the sensitivity matrices for the states and output respectively. In each matrix, the (i, j) element is defined as the partial derivative of the i-th state to the j-th parameter:

$$s_{i,j}(t) = \frac{\partial x_i(t)}{\partial \theta_j}. \tag{10}$$

With these variables, we now define an additional ODE system for the sensitivity equations:

$$\dot{S}_{\mathbf{x}} = \frac{\partial \boldsymbol{f}}{\partial \mathbf{x}} S_{\mathbf{x}} + \frac{\partial \boldsymbol{f}}{\partial \boldsymbol{\theta}}, \quad S_{\mathbf{x}}(0) = S_{\mathbf{x}0} \tag{11}$$

$$S_{\mathbf{y}} = \frac{\partial \boldsymbol{h}}{\partial \mathbf{x}} S_{\mathbf{x}} + \frac{\partial \boldsymbol{h}}{\partial \boldsymbol{\theta}}. \tag{12}$$

To facilitate efficient and accurate Jacobian calculations during implementation, we use the CasADi automatic differentiation software [17]. The corresponding battery model and sensitivity ODEs are simulated within the CasADi framework using the IDAS solver developed and managed by SUNDIALS [18].

B. Parameter Selection

In [11], the Doyle-Fuller-Newman (DFN) is used to calculate parameter sensitivities for a library of inputs. The parameters are then ranked according to their orthonormalized sensitivity, where sensitivity is computed as $S_{\mathbf{y}}^T S_{\mathbf{y}}$ for each parameter. According to this sensitivity metric, we qualitatively picked an assortment of 6 parameters present in both the SPMeT and DFN that span the orthonormalized sensitivity spectrum. We chose some parameters ranked with "High" ($S_{\mathbf{y}}^T S_{\mathbf{y}} \geq 10e-2$), "Medium" ($10e-4 \leq S_{\mathbf{y}}^T S_{\mathbf{y}} \leq 10e-2$), and "Low" sensitivity ($S_{\mathbf{y}}^T S_{\mathbf{y}} \leq 10e-4$) magnitudes. Note that because the model is nonlinear in the parameters, there are no theoretical guarantees of parameter identifiability. However, higher sensitivity magnitudes indicate a higher chance of recovering the true parameter values from the available input data.

C. Parameter Estimation: Nonlinear Least Squares

After screening and selecting the optimal voltage response data according to sensitivity content, we formulate a nonlinear least squares problem to simultaneously estimate the 6 selected parameters:

$$\underset{\hat{\boldsymbol{\theta}}}{\text{minimize}} \quad \sum_{i=1}^{M} \left\| \mathbf{y_i}(t) - \hat{\mathbf{y}}_\mathbf{i}(t; \hat{\boldsymbol{\theta}}) \right\|_2 \tag{13}$$

where M is the number of input profiles selected in a batch of battery data, $\mathbf{y_i}$ is the experimentally measured voltage, and $\hat{\mathbf{y}}_\mathbf{i}(\mathbf{t}; \hat{\theta})$ is the model's predicted voltage.

IV. SIMULATION APPROACH

The parameter estimation framework is evaluated with a "model-to-model" comparison. The full-order DFN model is used to generate truth data. We simulate 5 "batches" of data, meant to represent 5 weeks of electric vehicle operation. Each batch contains 6 drive cycle data sets. Each drive cycle (DC1, DC2, LA92, SC04, UDDS, US06) represents a different driving scenario in terms of duration, distance, starts/stops, average and max currents, etc. In each successive batch, the true parameter values are manually perturbed by -5% in order to emulate aging. We estimate the 6 selected parameters from the DFN model with the initial guess perturbed from the truth model's parameters by 30% (see Table I), to imitate uncertainty in our initial parameter guess.

For each batch, the parameter estimation framework computes the sensitivity trajectories for all 6 drive cycles using the reduced-order SPMeT model. Then, it selects the 3 drive cycles with the highest sensitivity content. Here, we arbitrarily defined a data budget of 3 drive cycles. Next, the framework simultaneously estimates the 6 selected parameters in the full-order model using these cycles. In this study, the 3 selected drive cycles (LA92, SC04, UDDS) are the same over the 5 batches; hereafter, we refer to this set collectively as the training data set. We further validate our parameter estimation performance by using the parameter values identified in each batch to simulate a validation data set—the 3 drive cycles not used for parameter estimation (DC1, DC2, US06)—and compare to the truth model.

V. RESULTS & DISCUSSION

A. Sensitivity Computation Comparison

We evaluate the ability of the reduced sensitivity equations to approximate the sensitivity trajectories of the higher-order DFN model by performing a correlation analysis. Figure 3(a) plots the SPMeT and DFN normalized sensitivity value pairs (x: SPMeT, y: DFN). Each data point indicates the normalized sensitivity for a given parameter and drive cycle. The correlation coefficient $R = 0.996$ indicates that the sensitivity computed between the SPMeT and DFN is highly correlated for this study. Furthermore, as indicated by the marker coloring, the sensitivity for each parameter and relative sensitivity ranking of all the parameters is consistent across both models.

The high degree of correlation suggests that the SPMeT can be used to approximate sensitivity for the higher-order DFN model. We emphasize that we cannot claim this level of correlation holds for all combinations of parameter values and inputs. Given the local, not global nature of the sensitivity calculations, it is possible that the correlation does not hold away from the nominal parameter value.

To better understand whether the correlation holds beyond this simulation study, we performed the same analysis across 560 different input profiles. The current input types include charging/discharging/both for pulse, sinusoid, and constant current profiles (see [11] for more details). The resulting correlation trend is shown in Figure 3(b). The correlation coefficient $R = 0.842$ indicates that the correlation between the two models still holds but more weakly than for the previous simulation study. This result suggests that reduced sensitivity equations should work well, but there may be cases where the approximation deviates.

Of practical consideration, the computational time for simulating each model's sensitivity varies dramatically. For this simulation study, where the sensitivity trajectories for 6 parameters and 6 drive cycles were computed on a high-performance parallel computing resource, the wallclock time for the SPMeT was 53 seconds; the wallclock time for the DFN was 3.6 hours. This discrepancy highlights the potential value of being able to approximate a higher-order battery model's sensitivity with a lower-order model. Furthermore, the full-order model becomes increasingly intractable for more complex scenarios, given that the computational time scales non-linearly with the number of parameters and length/number of inputs being considered.

B. Parameter Estimation Performance

Final estimated parameter values are reported in Table I alongside the initial guess. The parameter estimation performance is evaluated according to the following metrics: (1) voltage root-mean-square-error (RMSE) and (2) internal state RMSE.

1) Voltage RMSE: Voltage RMSEs are plotted for the training and validation data sets in Figure 4. Each subfigure contains two curves: the red and blue curves denote the RMSE before and after (respectively) the parameters are optimized to reduce the RMSE. As can be seen, both models reduce voltage RMSE (from red curve to blue curve) below 1 mV and maintain a 1 mV voltage RMSE across the duration of the 5 batches. Note that the most significant accuracy improvement comes after batch 1, where the initial parameter guesses are offset by 30%. These results are to be expected since the parameter estimation optimization problem defines a cost function which explicitly minimizes voltage RMSE.

TABLE I: SPMeT / DFN Model Parameters

Parameter	Description	Value	Initial Guess	Final Value
R_s^+	Particle Radius (Cathode)	10E-6	14E-6	8.8E-6
κ	Electrolyte Conductivity	1.0	1.3	1.3
ε_e^-	Volume Fraction (Anode)	0.30	0.39	0.25
t_+	Transference Num.	0.38	0.49	0.45
R_f^+	Film Resistance (Cathode)	1.0E-4	1.3E-4	1.8E-4
R_f^-	Film Resistance (Anode)	5.0E-4	6.5E-4	2.9E-4

2) Internal State Errors: Note that we fit the parameters to minimize voltage error. As a result, we should not necessarily expect the internal state error to also be minimized. This turns out to be the case for both the training set and the validation set. Figure 5 illustrates the internal state mismatch between the models for several states of interest. Each state's RMSE is normalized by the max absolute value of the DFN truth model. The internal state error increases with each batch, despite re-fitting parameters to voltage for each batch. Importantly, many of these states are related to safety endpoints. The side reaction overpotential, η_s, for example, is critical for estimating the onset of lithium plating [19].

In Figure 6, we illustrate the relationship between the objective function and state error (here electrolyte concentration at the current collector) as a function of 2 parameters, by simulating the DFN for 20 discrete values. We see that the trough of local minima in the objective function (a) do not correspond to local minima in the state error (b). Thus, we can see graphically that even in a simpler 2-parameter case, the parameters may converge to values that lead to low voltage estimation error value and non-zero state estimation error. Given that this issue already manifests when varying 2 parameters, the problem can only worsen when more parameters are identified.

VI. CONCLUSION

This paper analyzes the problem of online parameter estimation in an electrochemical Li-ion battery model. The first key conclusion from this work is that the lower-order SPMeT approximates sensitivity well for the DFN. This finding is useful for online parameter estimation, where it has been shown that sensitivity data can be leveraged to improve identification performance. The second key conclusion from this work is that estimating parameters in electrochemical

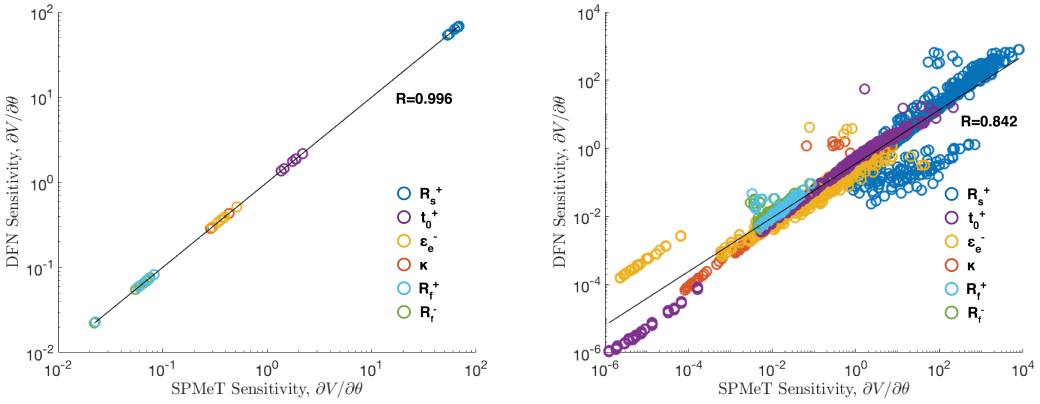

(a) (b)

Fig. 3: (a) DFN vs. SPMeT normalized sensitivity values. Each marker indicates the normalized sensitivity $\frac{\partial V}{\partial \theta_i}$ computed for each one of the six drive cycles and a given parameter. The six different marker colors correspond to the six parameters of interest in this simulation study. $R = 0.996$ indicates that the local sensitivities between the models are highly correlated. (b) The same DFN-SPMeT correlation analysis across 560 varying input profiles. The current input types include charging/discharging/both for pulses, sinusoids, constant current profiles. $R = 0.842$ indicates that the correlation holds well across a wider range of inputs but more weakly than in the drive-cycle simulation study.

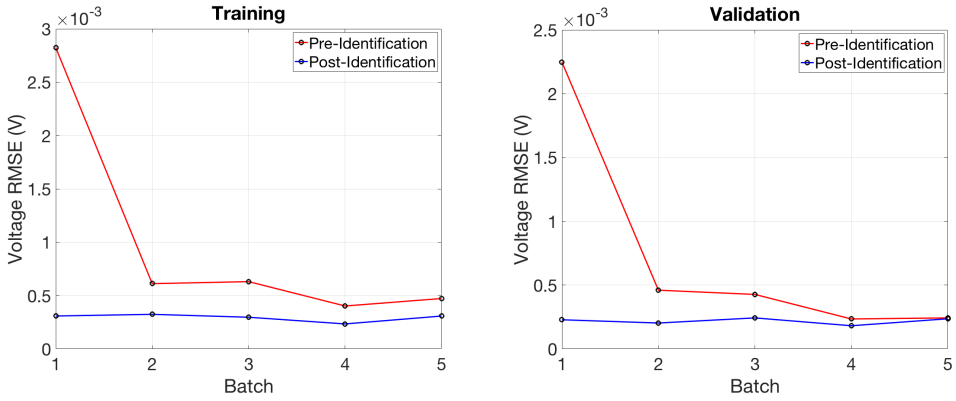

(a) (b)

Fig. 4: Voltage RMSE before and after parameter identification for (a) training data (b) validation data. In both data sets, voltage RMSE is reduced to below 1 mV and is maintained below 1 mV across the 5 batches.

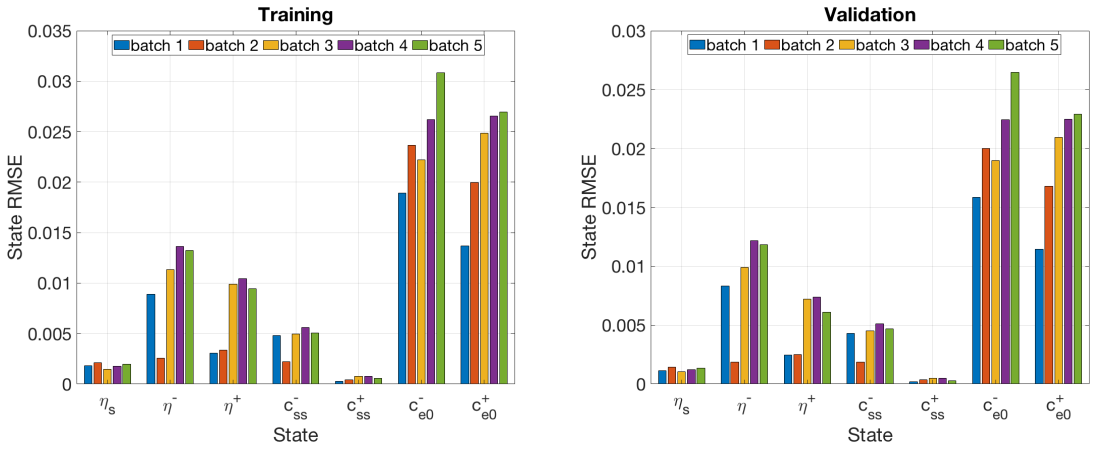

(a) (b)

Fig. 5: State RMSE after parameter identification for (a) training data and (b) validation data. For comparison purposes, RMSE values for each parameter are normalized by the maximum absolute state value of the truth model.

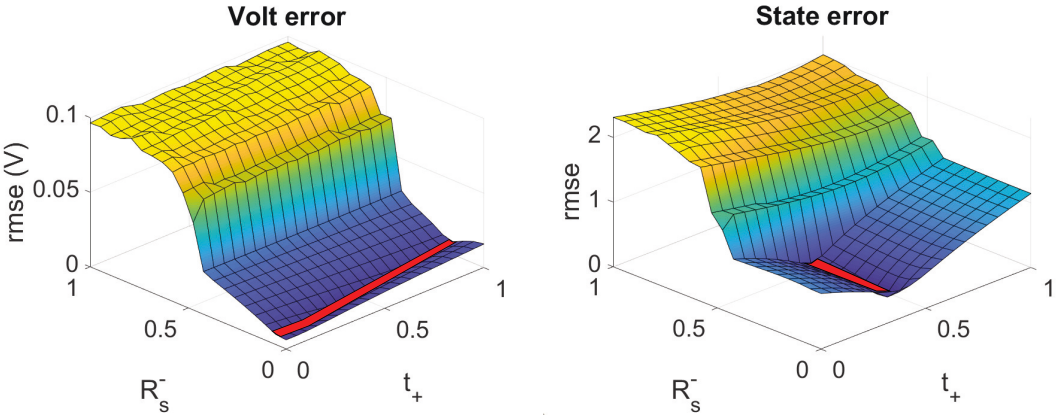

(a) (b)

Fig. 6: Surface plots of voltage RMSE (a) and internal state RMSE (b) as 2 DFN parameters are varied from a nominal truth value. The troughs of points within a small tolerance of the minimum have been marked in red. The parameters were discretized over 20 possible values each.

models based on an objective function that only considers voltage error can lead to inaccurate state predictions. This finding motivates the need for a modeling and estimation approach that simultaneously reduces voltage error while regulating internal state error. Ongoing work is focused on finding a tractable solution to this problem.

Acknowledgment

This material is based upon work supported by the National Science Foundation Graduate Research Fellowship Program under Grant No. DGE 1752814. Any opinions, findings, and conclusions or recommendations expressed in this material are those of the author(s) and do not necessarily reflect the views of the National Science Foundation. This research used the Savio computational cluster resource provided by the Berkeley Research Computing program at the University of California, Berkeley (supported by the UC Berkeley Chancellor, Vice Chancellor for Research, and Chief Information Officer).

References

[1] J. C. Forman, S. J. Moura, J. L. Stein, and H. K. Fathy, "Genetic identification and fisher identifiability analysis of the doylefullernewman model from experimental cycling of a lifepo4 cell," *Journal of Power Sources*, vol. 210, pp. 263 – 275, 2012.

[2] A. P. Schmidt, M. Bitzer, Á. W. Imre, and L. Guzzella, "Experiment-driven electrochemical modeling and systematic parameterization for a lithium-ion battery cell," *Journal of Power Sources*, vol. 195, no. 15, pp. 5071–5080, 2010.

[3] X. Hu, D. Cao, and B. Egardt, "Condition monitoring in advanced battery management systems: Moving horizon estimation using a reduced electrochemical model," *IEEE/ASME Transactions on Mechatronics*, vol. 23, no. 1, pp. 167–178, 2017.

[4] S. Dey, B. Ayalew, and P. Pisu, "Combined estimation of state-of-charge and state-of-health of li-ion battery cells using smo on electrochemical model," in *2014 13th International Workshop on Variable Structure Systems (VSS)*. IEEE, 2014, pp. 1–6.

[5] B. Saha, S. Poll, K. Goebel, and J. Christophersen, "An integrated approach to battery health monitoring using bayesian regression and state estimation," in *2007 IEEE Autotestcon*. Ieee, 2007, pp. 646–653.

[6] D. J. MacKay, "Information-based objective functions for active data selection," *Neural computation*, vol. 4, no. 4, pp. 590–604, 1992.

[7] D. Arengas and A. Kroll, "Removal of insufficiently informative data to support system identification in miso processes," in *2018 European Control Conference (ECC)*, June 2018, pp. 2842–2847.

[8] X. Lin, "A data selection strategy for real-time estimation of battery parameters," in *2018 Annual American Control Conference (ACC)*. IEEE, 2018, pp. 2276–2281.

[9] Q. Lai, S. Jangra, H. J. Ahn, G. Kim, W. T. Joe, and X. Lin, "Analytical sensitivity analysis for battery electrochemical parameters," in *2019 American Control Conference (ACC)*. IEEE, 2019, pp. 890–896.

[10] A. Pozzi, G. Ciaramella, S. Volkwein, and D. M. Raimondo, "Optimal design of experiments for a lithium-ion cell: parameters identification of an isothermal single particle model with electrolyte dynamics," *Industrial & Engineering Chemistry Research*, vol. 58, no. 3, pp. 1286–1299, 2018.

[11] S. Park, D. Kato, Z. Gima, R. Klein, and S. Moura, "Optimal experimental design for parameterization of an electrochemical lithium-ion battery model," *Journal of The Electrochemical Society*, vol. 165, no. 7, pp. A1309–A1323, 2018.

[12] M. J. Rothenberger, D. J. Docimo, M. Ghanaatpishe, and H. K. Fathy, "Genetic optimization and experimental validation of a test cycle that maximizes parameter identifiability for a li-ion equivalent-circuit battery model," *Journal of Energy Storage*, vol. 4, pp. 156–166, 2015.

[13] S. J. Moura, F. B. Argomedo, R. Klein, A. Mirtabatabaei, and M. Krstic, "Battery state estimation for a single particle model with electrolyte dynamics," *IEEE Transactions on Control Systems Technology*, vol. 25, no. 2, pp. 453–468, 2016.

[14] H. Perez, S. Dey, X. Hu, and S. Moura, "Optimal charging of li-ion batteries via a single particle model with electrolyte and thermal dynamics," *Journal of The Electrochemical Society*, vol. 164, no. 7, pp. A1679–A1687, 2017.

[15] K. E. Thomas, J. Newman, and R. M. Darling, "Mathematical modeling of lithium batteries," in *Advances in lithium-ion batteries*. Springer, 2002, pp. 345–392.

[16] P. A. Ioannou and J. Sun, *Robust Adaptive Control*. Upper Saddle River, NJ, USA: Prentice-Hall, Inc., 1995.

[17] J. A. E. Andersson, J. Gillis, G. Horn, J. B. Rawlings, and M. Diehl, "CasADi – A software framework for nonlinear optimization and optimal control," *Math. Program.*, In Press, 2018.

[18] A. C. Hindmarsh, P. N. Brown, K. E. Grant, S. L. Lee, R. Serban, D. E. Shumaker, and C. S. Woodward, "SUNDIALS: Suite of nonlinear and differential/algebraic equation solvers," *ACM Transactions on Mathematical Software (TOMS)*, vol. 31, no. 3, pp. 363–396, 2005.

[19] S. Lucia, M. Torchio, D. M. Raimondo, R. Klein, R. D. Braatz, and R. Findeisen, "Towards adaptive health-aware charging of li-ion batteries: A real-time predictive control approach using first-principles models," in *2017 American Control Conference (ACC)*. IEEE, 2017, pp. 4717–4722.